Dielectric Metamaterials Based on Electric and Magnetic Resonances of Silicon Carbide Particles

Jon A. Schuller,[1,*] Rashid Zia,[2] Thomas Taubner,[1] and Mark L. Brongersma[1]

[1]*Geballe Laboratory for Advanced Materials, 476 Lomita Mall, Stanford, California 94305, USA*

[2]*Division of Engineering, Box D, 182 Hope St., Brown University, Providence, Rhode Island 02912, USA*

(Received 21 May 2007; published 7 September 2007)

Silicon carbide particles exhibit both electric and magnetic optical resonances, allowing unexplored dielectric metamaterial designs. Experimental extinction spectra and Mie theory calculations of single microscale rod-shaped particles reveal three observable midinfrared resonant modes. Two of the modes are degenerate, with a frequency that can be tuned according to a resonance condition derived within the Letter. The existence of both electric and magnetic resonances may enable a novel negative refractive index metamaterial design.

DOI: 10.1103/PhysRevLett.99.107401 PACS numbers: 78.20.Ci, 42.25.Bs, 71.36.+c, 78.30.−j

The resonant interaction of light with particles of subwavelength dimension has important consequences for many areas of modern research. For instance, periodic or random ensembles of small particles can be used to form artificial materials that respond to light in a unique and carefully designed fashion. In these so-called metamaterials, an effective permittivity and permeability are generated by superimposing the microscopic responses of individually designed "meta-atoms." When both the effective permittivity and permeability are negative, the structure will possess a negative index of refraction [1], enabling a variety of novel optical applications [2]. In most realizations of negative index metamaterials (NIM), the constituent subunits are formed of metallic materials. Engineering the requisite magnetic response requires sophisticated building blocks designed to mimic subwavelength resonant *LC* circuits: split ring resonators [3] or paired rods [4], for instance. In contrast, generating an electric response can be accomplished with simpler metallic structures, such as uncoupled rods or strips [5]. By combining these distinct elements properly, metallic metamaterials may simultaneously display negative electric and magnetic responses and thus a negative refractive index.

At midinfrared frequencies, silicon carbide (SiC) is an interesting alternative to metals. The relative permittivity of SiC exhibits a sharp resonance near 800 cm^{-1} (12.5 μm) due to excitation of transverse optical phonons [6] [Fig. 1(a)]. At the high frequency side of this resonance, the dielectric function is negative, and the optical response is similar to metals. Analogous to the surface plasmon-polaritons supported by metals, localized surface *phonon*-polariton modes in SiC structures have enabled applications in sensing, such as enhanced spectroscopy [7] and near field microscopy [8]. However, unlike metals which exhibit a free electron resonance ($\varepsilon \rightarrow -\infty$) at dc frequencies ($\omega \rightarrow 0$), the SiC phonon resonance occurs at a finite frequency. This allows for a low frequency regime where the permittivity is large and positive with moderate damping, a fact particularly relevant to metamaterial design. For instance, large permittivity spherical particles can generate negative effective permeabilities at frequencies near a magnetic dipole resonance [9]. When the sphere radius is increased, such particles can also exhibit an electric dipole resonance. Thus, using spheres of two distinct sizes, one can simultaneously excite both resonances and create an isotropic negative index metamaterial (NIM) comprised solely of dielectric particles [10]. Similar studies of rod-shaped particle arrays have focused on the negative permeability arising from a magnetic-type resonance [11,12]. In contrast to complex metallic elements, spherical and cylindrical particle resonances can be described analytically using Mie theory [13]. In this Letter, we show that positive permittivity rod-shaped SiC particles exhibit *both* electric and magnetic Mie resonances and investigate the implications for metamaterial design.

We present experimental and theoretical extinction spectra of single whisker-shaped SiC particles which are subwavelength in diameter but many wavelengths long. We identify three resonant modes supported by such particles and determine the metamaterial response generated by each distinct mode. The single particle measurements reveal polarization and size effects that are obscured in ensemble measurements, facilitating comparison with analytical Mie calculations for scattering from infinitely long cylinders. Dominant features in the experimental extinction spectra are attributed to resonant excitation of discrete

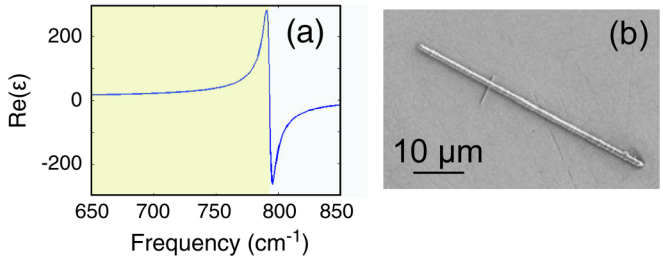

FIG. 1 (color online). (a) Real part of the silicon carbide dielectric function using an oscillator model reported in Ref. [8]. The highlighted portion shows the frequency range studied in this Letter. (b) Scanning electron micrograph of a SiC whisker.

transverse electric (TE) and transverse magnetic (TM) modes. We derive a simplified resonance condition for these modes, which is experimentally verified through a systematic study of various differently sized whiskers. Finally, we show that the zeroth (first) order TM mode can generate a resonant permittivity (permeability) and propose combining the two resonances to form a novel, easily fabricated NIM.

In our experiments, cubic (β) phase SiC whiskers manufactured by Alfa Aesar were washed in ethanol and dispersed onto a zinc selenide (ZnSe) substrate. Whisker dimensions typically varied between 1 and 2 μm in diameter and between 40 and 100 μm in length. A scanning electron micrograph (SEM) of a typical whisker is shown in Fig. 1(b). Transmission measurements were performed using a Fourier-transform infrared spectrometer (Nicolet 6700) coupled to a microscope (Continuum XL). A LN_2-cooled mercury cadmium telluride detector measures the light intensity transmitted through a sample area defined by a focal plane aperture. Ensemble measurements [Fig. 2(a)] show strong extinction (scattering plus absorption) within the frequency range of interest. However, to investigate size and polarization effects, it is necessary to make single particle measurements. Polarized extinction spectra of a typical whisker [1 μm diameter, Fig. 1(b)] are presented in Fig. 2(a). For TM polarization (E field parallel to the whisker's long axis), a sharp peak in extinction at 774 cm^{-1} is observed, superimposed on a broader low frequency peak. For TE polarization (E field perpendicular to long axis), there is a similar sharp peak at 785 cm^{-1} but the extinction at low frequencies is featureless. The experimental spectra exhibit three distinct peaks, two of which are nearly degenerate.

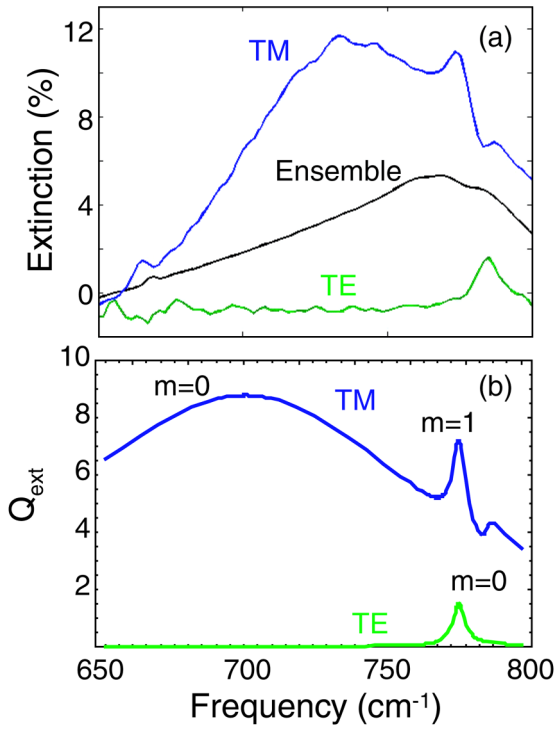

FIG. 2 (color online). (a) Ensemble, TM (E field parallel to long axis) and TE (E field perpendicular to long axis) polarized extinction spectra of a 1 μm diameter whisker. (b) Calculated extinction efficiency of an infinitely long 1 μm diameter SiC cylinder for both TE and TM illumination. The spectrum shows features attributable to three distinct modes.

To evaluate the origins of these resonances, experimental spectra are compared to calculations based on Mie theory for infinitely long cylinders [13]. We perform our calculations for normal incidence illumination where the illuminating, scattered, and interior fields can be considered purely TE or TM. The scattered fields are decomposed into a cylindrical basis set of discrete modes indexed by their azimuthal phase dependence $e^{im\varphi}$, with TE and TM coefficients

$$a_m = \frac{nJ'_m(ka)J_m(nka) - J_m(ka)J'_m(nka)}{nJ_m(nka)H'_m(ka) - J'_m(nka)H_m(ka)}$$

$$b_m = \frac{J_m(nka)J'_m(ka) - nJ'_m(nka)J_m(ka)}{J_m(nka)H'_m(ka) - nJ'_m(nka)H_m(ka)},$$

where k is the free space wave vector, n is the particle's index of refraction, a is the cylinder radius, J_m is the mth order Bessel function of the first kind, H_m is the mth Hankel function of the first kind, and the primed variables are differentiated with respect to their arguments. The extinction spectra can be calculated directly once the a_m and b_m coefficients are known [13]. The calculated extinction efficiency, Q (extinction cross-section divided by physical cross-section), of a 1 μm diameter SiC cylinder is presented in Fig. 2(b). The calculations show good agreement with experiments. For TM polarization, both the calculated and experimental extinction are characterized by a broad low-frequency peak as well as a sharp peak centered near 777 cm^{-1}. The low frequency peak is redshifted relative to the experimental spectrum, a discrepancy which is most likely caused by off-normal rays coupled by the microscope objective [14]. For TE polarization, there is also a sharp peak at 777 cm^{-1}, superimposed on a flat background. The approximate degeneracy seen experimentally is strictly degenerate in the theoretical calculations. The subtle breaking of degeneracy observed in experimental spectra may result from experimental complications: the previously mentioned off-normal rays, the presence of a substrate, finite whisker length, or departure from a circular cross-section, for instance. Regardless, the analytical nature of Mie calculations clarifies the origins of the multiple features in the extinction spectrum and allows us to attribute each feature to a *single* mode. Our spectra are dominated by three different modes: TM_0, TM_1, and TE_0, where the subscript refers to the mode's m number.

Having identified discrete modes in the spectra, we examine the resonance conditions that determine their natural frequencies. For instance, in Fig. 2, we see that the TM_0 and TM_1 modes are resonant at the same frequency. Using appropriate Bessel function identities, it can

be shown that $a_0 = b_1$ irrespective of the frequency, particle size, refractive index, etc. The observed mode degeneracy reveals a very general property of scattering within cylindrical coordinate systems. This is particularly interesting since we can derive a general resonance condition for the higher order TM modes. Consider the b_m coefficients. When the denominator is close to zero, the coefficient becomes large causing a peak in extinction. The zeros occur when $J_m(nka)/J_m^{'}(nka) = nH_m(ka)/H_m^{'}(ka)$. Because of material losses, the index of refraction is a complex quantity. We assume, as is typical for dielectric resonators, that the resonance frequencies are determined primarily by the real part of the refractive index. For small diameter particles ($ka \ll 1$), the equality approximately reduces to

$$\frac{J_m(nka)}{J_m^{'}(nka)} = nka[\gamma - \frac{i\pi}{2} - \ln(2) + \ln(ka)]; \qquad m = 0$$

$$\frac{J_m(nka)}{J_m^{'}(nka)} = -\frac{nka}{m}; \qquad m > 0$$

where γ is Euler's constant. It is important to note that this is *not* an electrostatic approximation; the wavelength inside the particle is in fact comparable to the particle size. Because of the $\ln(ka)$ term in the first expression, finding the lowest order resonance frequency requires solving a complex transcendental equation. For higher order modes, however, the simplified resonance condition is purely a function of the "normalized radius" (nka) and can be solved [15], revealing that the $TM_{m>0}$ resonance occurs when $J_{m-1}(nka) = 0$. Thus, we have derived a considerably simplified resonance condition for the degenerate TM_1 and TE_0modes.

The resonance condition derived above is particularly helpful for engineering a desired spectral response. In our experiments, whisker size is an easily adjustable parameter. By varying the whisker diameter, we can tune the spectral response of our small particles. In Fig. 3, we show a quantitative comparison of our analytical calculations and experiment. Using the derived TM_1, TE_0 resonance condition, we calculate the resonant particle size as a function of frequency. The calculated values are compared to values taken from experimental, unpolarized extinction spectra of various sized whiskers on both ZnSe ($\varepsilon = 5.76$) and silicon ($\varepsilon = 11.6$) substrates. We see good agreement between theory and experiment for small whisker diameters, with no observable substrate effect. By varying its size, we can shift a particle's frequency dependent electromagnetic response in an easily understood fashion.

In a metamaterial, we can expect the macroscopic response of a structure to reflect characteristics of the individual particle resonances. Consider the TE_0 mode, which is characterized by a strongly resonant magnetic field directed along the cylinder axis. In Ref. [11], O'Brien and Pendry showed that a TE illuminated array of large permittivity cylinders would possess a negative effective permeability near the TE_0 resonance frequency. The superposition of enhanced magnetic fields arising from each cylinder mimics a bulk, macroscopic, material response. The authors used a homogenization procedure [16] that defines the effective permeability (permittivity) as the ratio of two quantities: an average of the B (D) field over a unit cell face, and the H (E) field over a unit cell edge. In their work, the full numerical calculations showed excellent agreement with a simplified analytical model derived from the Mie solutions for a single cylinder [17]. Using an identical value for the ratio of cylinder radius to spacing (0.4), we evaluate their analytical expression and calculate the effective permeability of a TE illuminated square lattice of 1.5 μm diameter (note a change in whisker size relative to Fig. 2 [18]) SiC cylinders [Fig. 4(a)]. The effective permeability exhibits a resonance near, but not exactly equal to, the mode frequency.

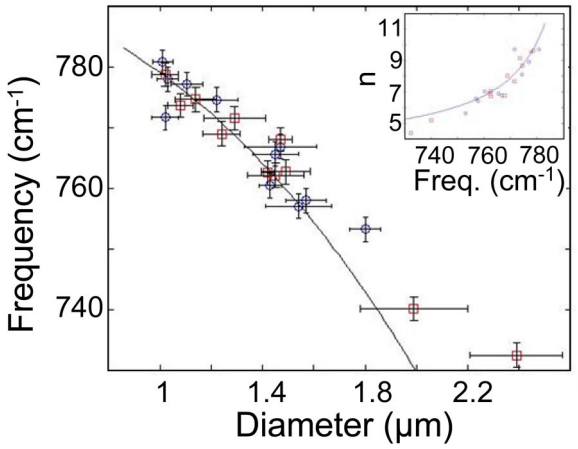

FIG. 3 (color online). Experimentally determined TM_1 resonance frequency versus particle size, extracted from unpolarized extinction spectra of whiskers on ZnSe (squares) and Si (circles) substrates. Whisker diameters are measured in a SEM at 15 points along the whisker axis and then averaged. Horizontal error bars give the measured standard deviation. Vertical error bars are given by the instrument resolution (± 2 cm^{-1}). Experimental values are compared to values calculated assuming the simplified resonance condition ($nka = 2.4$) described in the text. Inset: the same data, plotted as refractive index (n) versus frequency.

Considering the multiple modes in our experimental and theoretical extinction spectra, we predict a number of previously unexplored metamaterial applications. For instance, we can compare the TM_0 mode with the TE_0 mode discussed above. The electric field of one mode is identical to the magnetic field of the other, and vice versa. Hence, under TM illumination, we can expect a resonant permittivity due to excitation of the TM_0 mode [Fig. 4(b)]. Interestingly, the permittivity resonance is shifted by over 100 cm^{-1} relative to the mode frequency (the TM_0 resonance frequency for a 1.5 μm cylinder is $\sim$630 cm^{-1}). Relative to the TE_0 mode, the much larger width of the TM_0 particle resonance causes a much larger blueshift in the calculated material parameter. The contribution of axial ($\hat{z}$) fields to the effective material constants is unique to the

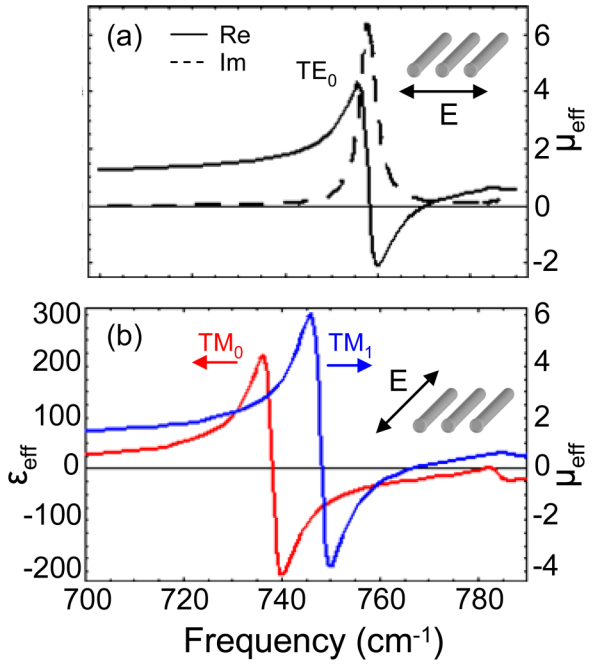

FIG. 4 (color online). (a) Calculated effective permeability for a normal incidence TE illuminated array of infinitely long 1.5 μm diameter SiC rods. (b) Calculated permittivity (permeability) due to excitation of the zeroth (first) order TM mode. Imaginary components have been omitted for clarity.

zeroth order modes. For higher order modes, the average value of the axial fields over a unit cell face is equal to zero [19]. To describe the influence of the TM_1 mode, then, we must consider the contribution of the magnetic fields, which point along the radial ($\hat{r}$) and azimuthal ($\hat{\varphi}$) directions. These components define a plane perpendicular to the cylinder axis, wherein the magnetic fields make a dipolelike pattern. Converting to Cartesian vectors and performing the homogenization procedure, we see that this mode generates a resonant permeability [Fig. 4(b)]. Of particular interest, the permeability is negative over a frequency range where the TM_0 mode causes a negative permittivity. Combining the two resonances, then, we can expect an array of SiC cylinders to possess a negative refractive index under TM illumination. Because of the cylindrical symmetry, the refractive index of such an array is nearly invariant to rotations about one axis. Furthermore, fabricating such rod arrays is easy, if one relaxes the requirement of a circular cross-section. Although more work is needed, the TM cylindrical particle resonances suggest intriguing new possibilities for midinfrared metamaterials.

In conclusion, we have observed and identified a number of discrete cylindrical modes supported by single SiC particles and shown how such modes may enable novel, partially isotropic, easily fabricated, dielectric metamaterial designs. Additionally, we demonstrated a mode degeneracy intrinsic to cylindrical geometries and derived a simplified resonance condition for the degenerate modes. Finally, although we have focused on Silicon Carbide and mid-IR frequencies, the concepts presented in this Letter are applicable to *any* strongly resonant dielectric system, allowing for similar physics at microwave [12] or visible [20] frequencies.

This work was funded by the Center for Probing the Nanoscale (CPN), an NSF NSEC, NSF Grant No. Phy-0425897. T. T. was supported by the Postdoc Program of the German Academic Exchange Service (DAAD).

Note added in proof.—After acceptance of our manuscript, we learned about a complementary paper [21] wherein researchers experimentally verify negative refraction in a TM illuminated array of large permittivity ceramic rods at microwave frequencies.

*Corresponding author: jonschuller@stanford.edu

[1] V. G. Veselago, Sov. Phys. Usp. **10**, 509 (1968).
[2] V. M. Shalaev, Nature Photonics **1**, 41 (2007).
[3] J. B. Pendry, A. J. Holden, D. J. Robbins, and W. J. Stewart, IEEE Trans. Microwave Theory Tech. **47**, 2075 (1999).
[4] V. A. Podolsky, A. K. Sarychev, and V. M. Shalaev, Opt. Express **11**, 725 (2003).
[5] J. B. Pendry, A. J. Holden, W. J. Stewart, and I. Youngs, Phys. Rev. Lett. **76**, 4773 (1996).
[6] E. D. Palik, *Handbook of Optical Constants and Solids* (Academic, Orlando, Fla., 1985).
[7] M. S. Anderson, Appl. Phys. Lett. **87**, 144102 (2005).
[8] R. Hillenbrand, Ultramicroscopy **100**, 421 (2004).
[9] M. S. Wheeler, J. S. Aitchison, and M. Mojahedi, Phys. Rev. B **72**, 193103 (2005).
[10] L. Jylha, I. Kolmakov, S. Maslovski, and S. Tretyakov, J. Appl. Phys. **99**, 043102 (2006).
[11] S. O'Brien and J. B. Pendry, J. Phys. Condens. Matter **14**, 4035 (2002).
[12] K. C. Huang, M. L. Povinelli, and J. D. Joannopoulos, Appl. Phys. Lett. **85**, 543 (2004).
[13] C. F. Bohren and D. R. Huffman, *Absorption and Scattering of Light by Small Particles* (Wiley and Sons, New York, NY, 1983).
[14] For light incident at the objective's maximal angle, calculations display a 20 cm-1 blueshift.
[15] Using the Bessel function identities $2J'_m(x) = J_{m-1}(x) - J_{m-1}(x)$ and $2mJ_m(x) = x[J_{m-1}(x) + J_{m-1}(x)]$.
[16] D. R. Smith and J. B. Pendry, J. Opt. Soc. Am. B **23**, 391 (2006).
[17] See Eq. (13) in Ref. [11].
[18] Compared to Fig. 2, we investigate larger diameter particles which show larger amplitude resonances.
[19] The integral of $e^{im\varphi}$ from 0 to 2π equals zero for $m \neq 0$.
[20] V. Yannopapas and N. V. Vitanov, Phys. Rev. B **74**, 193304 (2006).
[21] L. Peng *et al.*, Phys. Rev. Lett. **98**, 157403 (2007).